Color Centres and Polymorphism in Pure WO_3 and Mixed $(1-x)WO_{3-y}\cdot xReO_2$ Powders

E. Cazzanelli[1], G. Mariotto[2], C. Vinegoni[3], A. Kuzmin[4] and J. Purans[4]

[1]Istituto Nazionale per la Fisica della Materia and Dipartimento di Fisica, Università della Calabria, I-87036 Arcavacata di Rende (Cosenza), Italy

[2]Istituto Nazionale per la Fisica della Materia and Dipartimento di Fisica, Università di Trento, I-38050 Povo (Trento), Italy

[3]Dept. of Physics, GAP Optique, University of Geneva, Rue de l'Ecole de Medicine 3941 20, CH-1211 Geneva, Switzerland

[4]Institute of Solid State Physics, Kengaraga str. 8, LV-1063 Riga, Latvia

Abstract. The relationship between structural transformations and colour centres creation is discussed for deeply coloured hydrogen tungsten bronzes and for pure WO_3 powders, acquiring less intense colour after mechanical treatments of variable duration. A comparative study on coloration is made also for mixed compounds $(1-x)WO_{3-y}\cdot xReO_2$, where an evidence of a resonance effect for a particular Raman band at 970 cm^{-1}, attributed to the color centres, is observed. Besides, it is found that even moderate milling treatments result in a quite different structural evolution of tungsten trioxide upon cooling.

1. Introduction

Tungsten trioxide WO_3 is an important technological material widely known for its electrochromic and catalytic properties [1, 2]. Its performance as active electrode in electrochromic devices is derived from a combination of the following properties:

(i) The ability of tungsten ions to change their valence state upon reduction/oxidation processes both in the bulk and at the surface of crystalline grains [1,3]. In defect-free WO_3 single-crystals, the tungsten ions have the valence state 6+ with the 5d-shell being empty; these crystals are transparent with a band gap of about 3 eV at room temperature (RT) [1]. When the valence state of tungsten ions is reduced, the oxide turns to be blue coloured [1]. The colour centres are generally attributed [4] to defects consisting of electron excess charge, localised at the octahedra basic units $[W^{5+}O_6]$. The blue coloration can be induced by different methods such as chemical and electrochemical insertion [3,5] of small cations, UV irradiation [3,6,7] and annealing in vacuum [8]. Treatments inducing some degree of amorphisation of the crystalline structure, like ion beam bombardment [9], promote also the change of electronic distribution in the deformed regions and a consequent modification of its optical properties. Also, simple mechanical treatments like milling can induce the formation of electronically charged defects, as discussed in our previous works [10,11]. Many of these methods, however, generate a coloration which is easily reversed by simple exposure to an oxidising atmosphere. A different approach to obtain charged defects with specific optical absorption properties exploits the mixing of WO_3 with other oxides, having different electronic configurations: for example, an addition of even small fractions of rhenium oxide causes a strong coloration in the resulting mixtures after a proper thermal treatment [10,11]. Depending on the reduction method, the W^{5+} colour centres can be found in the bulk or at the surface of the crystalline grains. Moreover, depending on the concentration of such centres, the additional 5d-electron can be localised (small polaron) or smeared over a few (large polaron) or an infinite (conductive electron) number of tungsten ions [12]. Most work up to now was devoted

to the study of bulk colour centres with localised (as in amorphous thin films or glasses) or delocalised (as in tungsten bronzes) 5d-electrons [13].
(ii) Reasonable electronic [1,8,14] and ionic [1,12,13] conductivities allowing for the diffusion of the electrons balancing the insertion of foreign cations into the structure. In fact, the commercial powders exhibit n-type semiconductivity and show a yellow colour, due to the presence of bulk defects [14]. At high concentration of excess electrons the conductivity becomes metallic-like, and the heavily doped compounds M_xWO_3 (in most of the cases M = H, Li, Na) are labelled as "tungsten bronzes"[1,12,13]. The electronic conductivity, dependent on the charge carrier concentration, appears to be correlated also to the structural transformation of the crystal.

In the crystalline tungsten trioxide the change of the electronic density of states, responsible for the electrochromic effect, the electronic conductivity and the structural transformations are strongly correlated to each other. The crystal structure of WO_3 can be described as derivatives of an ideal cubic structure based on corner-sharing $[WO_6]$ octahedra, known as the ReO_3-type structure [12]. The different degrees of distortion with respect to the ideal cubic structure are caused by the second order Jahn-Teller effect [12, 15], reflecting an interplay between the lattice phonons and the electronic bands.

The increasing thermal motion of the atoms induces an isotropy of the structure, starting from very low symmetry triclinic or monoclinic phases up to the tetragonal phase; a true cubic structure is not stable for the pure WO_3 compound at any temperature below the melting point. On the basis of reported experimental data, the following sequence of crystal phases, in the order of increasing temperature, is presently accepted for the bulk crystal: monoclinic (II) polar or ε-phase with space group Pc (C_s^2), from 5 K to 278 K [16]; triclinic or δ-phase, $P\bar{1}$ (C_i^1), from 248 K to 290-300 K [16-19]; monoclinic (I) or γ-phase, $P2_1/n$ (C_{2h}^5), from 290-300 K to 600 K [17,19-21]; orthorhombic $Pmnb$ (D_{2h}^{16}), from 600 K to 1010 K [22]; tetragonal $P4/nmm$ (D_{4h}^7), from 1010 K to the melting temperature (1746 K) [23].

The insertion of excess electrons in WO_3, induces structural modifications leading to an evolution from lower to higher symmetry phases, quite similar to that obtained by increasing temperature. The phase transitions at low temperatures seem to be affected by much lower concentration of excess electrons. The polymorphism of WO_3 at RT and below is also remarkably affected by factors like the preparation route, the crystal size and the sample's history [11,24], while high temperature phases, on the contrary, show a good reproducibility of the results, lower hysteresis effects and independence of the phase sequence from impurities or mechanical treatments.

The amount of the reduced tungsten ions, induced by various methods, strongly affects the physical properties of WO_3. The study of such centres is of strong interest from both fundamental and applied points of view. In the past, the W^{5+} centres were mainly probed by electron spin resonance (ESR) technique, optical absorption and x-ray photoelectron spectroscopy (XPS) [1]. All these three methods provide mainly informations on the electronic structure of the colour centres, whereas their direct structural investigations are usually difficult, because of the small concentration of the reduced sites compared to the total number of tungsten ions. Therefore, one can expect to elucidate more by using a combination of different direct and indirect structural techniques applied to the same samples.

The principal aim of the present work is to discuss the production of colour centres and the structural transformations induced by means of various milling treatments. In particular, the paper will be focused on the transformations associated with colour changes, and will compare these optical, structural and vibrational changes with those induced by the high temperature mixing of tungsten oxide with rhenium oxide.

2. Experimental Methods

The starting material for the present study was commercial stoichiometric WO_3 powder („Reahim", Russia) for optical industrial applications with a nominal purity of 99.998 %. The powder had pale yellow colour with an average grain size of the order of microns: it will be identified in the following as *virgin powder.* The powders, manually compressed in a mortar of agate for a few minutes, will be labelled as *treated powders.* Finally, the powder treated for 1 h in a ball milling machine (Retschmuele) will be referred to as *ground powder.*

A set of "mixed powders" was produced by high-temperature (up to 600 °C) cumulative treatment from different mixtures of WO_3 and ReO_3: they can be simply identified by a general formula $(1\text{-}x)WO_{3\text{-}y} \cdot xReO_2$ where the index x denotes the relative molar fraction of rhenium ions and the index y reflects the non-stoichiometry of the material (note that ReO_2 appears as a result of the ReO_3 decomposition at about 400 °C). Following this pro-

cedure, seven compositions were obtained, whose colour varied from greyish-blue to black. The x values determined from the ratio of the W and Re L_3-edge x-ray absorption spectra edge jumps were found to be 0.05, 0.11, 0.17, 0.21, 0.24, 0.51 and 0.81. The phase content was confirmed by powder x-ray diffraction measurements.

Finally, hydrogenated samples used for comparison with the high-temperature WO_3 crystal transformations indicated by the general formula H_xWO_3, were prepared by H^+ insertion into the virgin WO_3 powder placed in 1N aqueous solution of sulphuric acid in the presence of indium as a catalyst. The hydrogen content was estimated by comparison of x-ray powder diffraction patterns for our samples with that available in the literature [25,26]. The as-prepared samples had deep-blue colour and the composition x = 0.23 corresponding to the tetragonal phase (JCPDF-ICDD 20-483). Upon hydrogen loss, they transformed first into the orthorhombic H_xWO_3 phase, with x = 0.1 (JCPDF-ICDD 6-210), and later turned into monoclinic (I) WO_3.

The samples were analysed by powder x-ray diffraction (XRD) and Raman spectroscopy. A Bragg-Brentano x-ray diffractometer, made by ItalStructures, working with Cu K_α radiation was used. The x-ray diffractograms were recorded at RT in the angle range 2θ = 20-65° and a step $\Delta(2\theta) = 0.05°$.

The RT Raman measurements were carried out in back-scattering geometry using a micro-Raman set-up, consisting of an Olympus microscope (model BHSM-L-2), mounting an objective 80× with a numerical aperture $N_A = 0.75$, and coupled to a 1 meter focal length double monochromator Jobin-Yvon (Ramanor, model HG2-S) equipped with holographic gratings (2000 grooves/mm). The spectral resolution was of the order of 3 cm^{-1}. The scattered radiation was detected by a cooled (-35 °C) photomultiplier tube (RCA, model C31034A-02), operated in photon counting mode. The signal was stored into a multichannel analyser and then sent to a microcomputer for the analysis. The standard macro-Raman configuration with a right angle scattering geometry and a liquid helium flux cryostat or an optical oven was used for low and high-temperature measurements, respectively. The Raman spectra were excited by the various wavelengths of a Krypton laser (647.1 nm and 530.9 nm), an Argon laser (mostly the 514.5 nm line, but for resonance measurements the higher energy lines also) and a He-Ne laser (632.8 nm). The light power entering the microscope was maintained below 10 mW, while in the macro-Raman configuration a nominal power of 20 mW were used. More experimental details can be found in [11,24,27].

3. Results and Discussion

3.1. Phase Transitions Caused by Temperature and Electron Insertion. The intercalation of small hydrogen ions into WO_3 allows to stabilize at RT high symmetry phases (orthorhombic, tetragonal and cubic), observed in the pure material well above RT. The insertion process results in the formation of the so-called hydrogen bronze H_xWO_3, having a modified electronic density of states of the host WO_3 matrix but, at the same time, not very much different crystal structure. Small hydrogen ions are distributed in H_xWO_3 among interstitial sites of the host crystal lattice and are weakly bound to the host structure allowing the good ionic mobility. The following phase sequence is reported for H_xWO_3 compounds: monoclinic (I) for $0 < x < 0.1$, orthorhombic for $0.1 < x < 0.15$, tetragonal B for $0.15 < x < 0.23$, tetragonal A for $0.23 < x < 0.5$ and cubic for $x > 0.5$ [25,26], quite similar to that of pure WO_3 for increasing temperatures [19-23].

The vibrational spectroscopy can provide very useful information on the phase transitions in WO_3, complementary to that obtained by diffraction techniques. Until now, Raman and IR spectroscopic studies have been widely used for the phases close to RT [28,29], but no data have been reported to our knowledge for the temperature-driven orthorhombic-to-tetragonal phase transition occurring at 740 °C in the pure oxide. In the following, comparative Raman investigations are presented on the changes of phonon spectra during the intercalation-induced and temperature-induced structural transformations.

Experimental problems exist for both types of measurements: at high temperatures, a strong broadening of bands and an increase of spurious contributions to the spectra make the analysis of the specific Raman peaks difficult; for the intercalated compounds, the optical absorption of the laser light, caused by the coloration, strongly decreases the Raman scattering cross section. In addition, a spontaneous loss of protons of the samples in the oxidising atmosphere does not allow for a quantitative control of the hydrogen molar fraction x, however, it is possible to follow the evolution from highly intercalated phases to less intercalated ones by performing several fast Raman spectra during the time of the de-intercalation process, even losing somewhat in terms of signal-to-noise ratio.

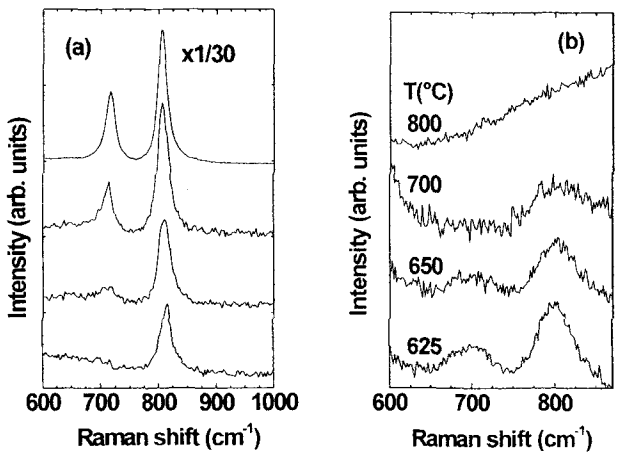

Fig. 1. (a) Evolution of the Raman spectra for H_xWO_3 upon oxidation in air. The starting H_xWO_3 powder with the maximum hydrogen content x = 0.23 is shown at the bottom. The top spectrum, reduced by a factor 30 to be comparable, was obtained after two hours of exposition to air and corresponds to pure monoclinic (I) WO_3. The intermediate spectra correspond to compositions in the range $0 < x < 0.23$. (b) Temperature dependence of the high frequency Raman modes for the tungsten trioxide WO_3 powder across the orthorhombic-to-tetragonal phase transition.

In our experiment, the maximum level of hydrogen insertion reached $x \approx 0.23$ as it was controlled by comparison with reported XRD patterns [25,26]: the hydrogen bronze $H_{0.23}WO_3$ appears to be deep-blue coloured being in the tetragonal phase. At increasing air exposition periods of time after hydrogenation, the powder returns back to the yellow monoclinic (I) WO_3 phase, passing through the orthorhombic H_xWO_3 ($0.1 < x < 0.15$). This process is reflected by the time sequence of the spectra in Fig. 1(a), starting from the maximum proton content $x \approx 0.23$, corresponding to the bottom spectrum and resulting in pure monoclinic (I) phase after two hours of measurements, corresponding to the top spectrum. The data acquisition for all spectra was started from the higher frequency side to avoid a bias in the 710 cm^{-1} mode to the 816 cm^{-1} mode intensity ratio, depressing the lower frequency mode upon the de-hydrogenation process. In fact, the 710 cm^{-1} mode decreases strongly with respect to the 816 cm^{-1} mode upon the hydrogen insertion, and disappears for proton concentrations lower than the maximum attainable.

In the case of the H_xWO_3 compound, a remarkable dependence is observed for the highest stretching mode frequency vs. the hydrogen content: upon de-hydrogenation, its frequency decreases from 814 cm^{-1} in $H_{0.23}WO_3$ to 806 cm^{-1} in monoclinic (I) WO_3. This mode hardening can be attributed to the change of the formal tungsten valence state: when protons are inserted, it is reduced to 5.77+ in $H_{0.23}WO_3$. Assuming that the reduced tungsten ions are the colour centres with polaronic absorption mechanism [30,31], the donated electron is localised at the tungsten ion sites increasing the covalency and thus the strength of the tungsten-oxygen bonds. Therefore, a different stretching frequency should be expected for the same distance. The experimental data show as net result a slight increase of the W-O stretching frequency, even taking into account a greater bond length in H_xWO_3 compared to WO_3.

The comparison of the same stretching modes evolution at high temperatures across the orthorhombic-to-tetragonal phase transition in pure WO_3 (Fig. 1(b)) suggests the strict similarity of the two transformations. Both stretching modes at 700 and 800 cm^{-1} are no more detectable at 800 °C, when the powders are in the tetragonal phase, but it is very interesting that the lower frequency mode at 700 cm^{-1} disappears already at temperatures below the transition point (740 °C), while the 800 cm^{-1} mode disappears in the tetragonal phase. This fact, however, can be due to peculiar experimental conditions, not to a complete symmetry change inhibiting all the Raman modes. The monotonically increasing contribution observed at 800 °C in Fig. 1(b) is probably due to blackbody radiation of the oven cavity or to luminescence contributions arising from the change of optical properties across the orthorhombic-tetragonal phase transition [30]. Some Raman active modes are expected to survive in the tetragonal phase [32], on the basis of the standard group theoretical analysis, but the anharmonic interactions, strongly enhanced by the high temperature, surely induce a dramatic broadening of the surviving Raman bands, and this fact, together with the spurious contributions, does not allow the detection of the 800 cm^{-1} stretching mode at $T \geq 800$ °C.

A reasonable explanation of the existence of only one stretching mode in the tetragonal phase [23] is the symmetrization of the W-O bonds in the *a-b* plane, while the bonds along the *c* axis remain different and Raman active. In fact, the total Raman spectrum of hydrogenated tungsten oxide shows a number (4) of Raman active modes lower with respect to the orthorhombic phase [28], but in agreement with the predictions of the group theory for the tetragonal phase.

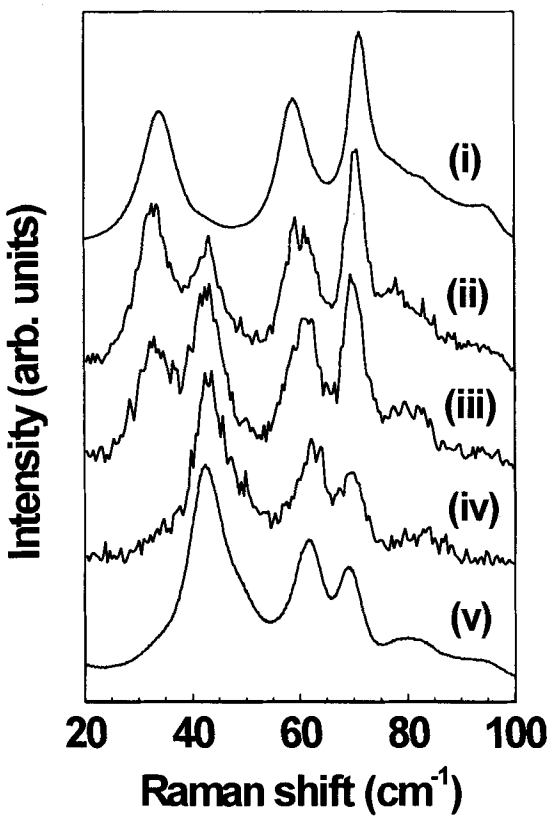

Fig. 2. Low frequency Raman spectra of WO_3 *virgin* powder samples undergoing cumulative mechanical pressure treatments for short times: i) starting *virgin* powder (γ-phase); ii) after 5 s compression; iii) after 10 s compression; iv) after 120 s compression; v) reference *treated* powder sample, after 10 minutes moderate milling (δ-phase).

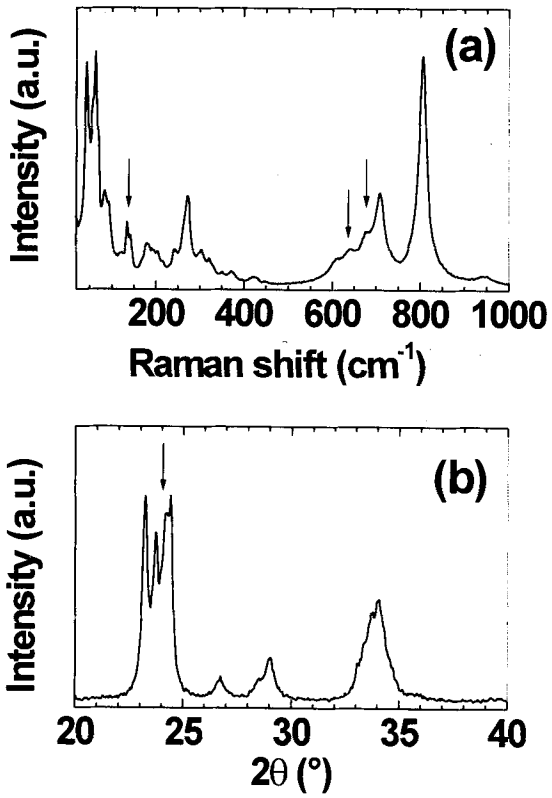

Fig. 3. Raman spectrum (a) and XRD pattern (b) of WO_3 *ground* powder after 1h milling. Arrows indicate the typical features of the monoclinic (II) ε-phase: (a) the bands at 143, 643 and 679 cm^{-1} and (b) the peak at $2\theta \approx 24°$.

3.2. Polymorphism Driven by Moderate Mechanical Treatments. The crystal structure of pure WO_3 is strongly affected by the mechanical treatments, even moderate. The most evident effect is the transformation of the powders from monoclinic to triclinic structure, under a weak grinding treatment at RT. It can be inferred from small modifications of the XRD patterns, but a clearer evidence is given by the evolution of low frequency bands (up to 100 cm^{-1}) of the Raman spectra. These bands correspond mostly to lattice modes of librational nature and are noticeably affected by the transitions between the low symmetry phases of WO_3, which involve mainly collective rotations of the basic [WO_6] octahedral units [18,23]. The Raman spectra modifications between the monoclinic (I) (γ-) and triclinic (δ-) phases are already known [33, 34]; in our powder samples they are well evident in Fig. 2 as a consequence of short-time manual treatments: the relative intensity of the 34 cm^{-1} peak (typical of the monoclinic phase) decreases whereas the peak at 41 cm^{-1} (typical of the triclinic phase) increases. Note that the phase transformation is reversible by annealing the sample well above RT.

A different phenomenology occurs when the mechanical treatments increase in both strength and duration. After a first transformation into the δ-phase, observed for mild mechanical treatments, at some step of the structural evolution (after about 1 h milling) new Raman peaks appear at 143, 643 and 680 cm^{-1} (Fig. 3(a)): they correspond to the ones of the low temperature monoclinic (II) ε-phase [34]. The occurrence of the ε-phase in these *ground powders* is also supported by XRD measurements, where a new diffraction peak appears at $2\theta \approx 24°$ (Fig. 3(b)). To our knowledge, a Raman evidence of ε-phase at RT was previously reported only for WO_3 microcrystals of size below 100 nm [35,36].

A high sensitivity of the phase occurrence to mechanical treatments is also found at low temperatures. The evolution of the high-frequency Raman bands in *virgin* and *treated* powders is shown in Fig. 4.

The *virgin* powder transforms into the new *N*-phase, whose characteristic modes (the most evident ones are at 684 and 790 cm^{-1}) are strongly dominant below 120 K

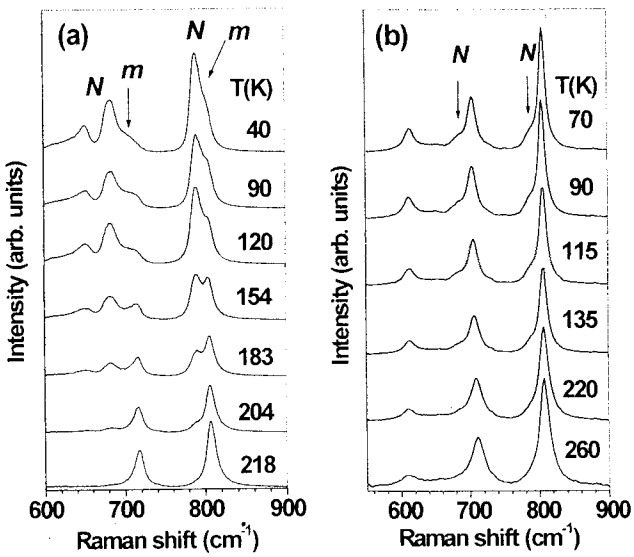

Fig. 4. Low temperature evolution of the high frequency stretching modes in Raman spectra of WO_3 (a) *virgin* and (b) *treated* powders. The monoclinic (I) γ-phase is labelled by *m* in (a). Shoulders attributed to the *N*-phase are indicated in the lowest temperature spectrum in (b). Temperature values are obtained from the Stokes/anti-Stokes ratio in all the cases.

(Fig. 4(a)), while the modes of the monoclinic (I) γ-phase (stable at RT) survive also as weak features or shoulders even at 40 K. Some modes having quite close frequencies to that of the *N*-phase were previously observed at low temperature in WO_3 microcrystals [35,36], grown by an evaporation method. It is interesting to note that there is no evidence of the monoclinic (II) polar ε-phase, previously reported by Salje et al. in single crystals at ~230 K [33,34] and in a polycrystalline sample at T < 220 K [16]. This absence, however, has been already reported by others studies on powder samples [33,37]. Moreover, in the present measurements no evidence was also found for the expected transition to the triclinic δ-phase. It has been observed, on the contrary, at low temperatures in most previous works [23,33,34].

The low temperature Raman spectra of the *treated* powder, being in the triclinic phase at RT, are shown in Fig. 4(b). It is quite evident that no dramatic change of the spectral shapes occurs in the explored temperature range, besides the usual broadening of the peaks with temperature. Even at the lowest temperature (70 K) the main spectral pattern corresponds well to that of the triclinic δ-phase observed at RT. However, the spectroscopic evidences for the *N*-phase are certainly detectable, but they appear much weaker than in *virgin* powders: the presence of the *N*-phase is revealed by the asymmetry of the low frequency side of the 712 and 808 cm^{-1} stretching modes. These bands are consistent with the satellite bands at 687 cm^{-1} and 787 cm^{-1}, reported by Hayashi et al. [35,36] at low temperatures on microcrystalline samples, and with the bands well observed in the *virgin* powder (Fig. 4(a)).

The findings of the transition to the *N*-phase in the *virgin* powder, having a much greater grain size than evaporated microcrystals, allows to rule out the hypothesis that the *N*-phase could be a peculiar characteristic of microcrystalline samples. Therefore, other variables, like the stress and carrier concentration (connected to substoichiometry), should play an important role in driving such transition and have to be carefully considered. The significantly low value of the W-O stretching frequency in the *N*-phase spectrum (790 cm^{-1} against more than 800 cm^{-1} for all the others phases) suggests a more relaxed structural configuration, which cannot be induced by simple lattice parameter contraction, usually obtained by temperature reduction or high pressure application. Thus, the *N*-phase and the ε-phase would represent opposite evolutions of the crystal structure, and we could expect that conditions promoting the transition to the *N*-phase inhibits the transition to the ε-phase and *vice versa*. Recently, we have suggested [24] that the ε-phase is favoured by the total strain generated by (bi)polarons when they reach a sufficient concentration, equivalent to the application of high pressure. Thus the evolution of WO_3 toward either the ε-phase or N-phase can be determined also by the carrier concentration, associated with oxygen deficiency. In fact, slightly defective WO_{3-x} samples show the transition to the ε-phase [9, 38], while the N-phase seems to be characteristic of crystals having a minimum amount of stress and very low carrier concentration.

3.3. *Coloration and Structural Disorder Caused by Strong Mechanical Treatments*. The prolonged time of milling results in deep-blue coloration of the *ground* WO_3 powders. The broadening of peaks in XRD patterns suggests an increase of structural disorder caused by a decrease of the crystallite size and an increasing strain. For very long times, up to 21 hours, the characteristic peaks of the various crystal phases become very hard to separate. The Raman scattering cross section strongly decreases, because of the defect-induced optical absorption, and no discrimination of the characteristic peaks for different phases is possible. However, the basic skeleton, common to all WO_3 phases derived from the ReO_3-type structure, survives, and a true "amorphisation" must be ruled out.

The Raman spectrum of the 1 h ground WO_3 powder

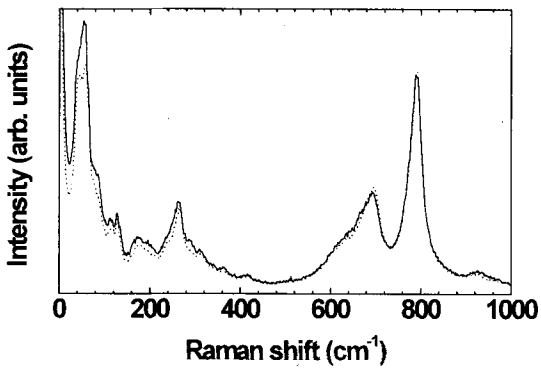

Fig. 5. Comparison between the Raman spectra of blue coloured *ground* powder just after 1 h milling (solid line) and the same powder returned back to yellow colour after an annealing treatment during 8 h at 90 °C (dotted line). The former spectrum has much lower intensity, so that the strong 800 cm^{-1} peak was used for normalization.

is shown in Fig. 5 by solid line. A particular Raman band, at about 950 cm^{-1}, not present in bulk crystal phases, may be attributed to the structural disorder and to the increasing fraction of surfaces when the grain size decreases. Similar bands appear also in crystalline $WO_3 \cdot nH_2O$ [29] and amorphous WO_3 [39] films and are usually assigned to a vibration of the W=O double bond involving terminal oxygen. It is important to remark that a moderate heat treatment in a normal oxidising atmosphere can easily reverse the blue coloration, and allows to restore the Raman scattering intensity generated by the powder samples. But the XRD patterns, as well as the Raman spectral shape remain those of disordered strained crystals after milling. In Fig. 5 such effect is well evidenced: the two Raman intensities, collected before and after the heating, have been normalised to the 800 cm^{-1} peak, and the spectral profiles overlap almost perfectly. In addition, the excitation of Raman spectra by different laser lines, ranging from the red light (near to the colour centre absorption band) to the blue light (far away from it), does not reveal any appreciable resonance effect, that allows to exclude association of the terminal bonds (and thus 950 cm^{-1} band) to the surface colour centres.

3.4. Colour Centres in Mixed Powders (1-x)$WO_{3-y} \cdot xReO_2$. The idea to introduce excess electrons in tungsten oxide by mixing with rhenium oxide has been tested by studying the coloration and the structural transformations in the mixtures $(1-x)WO_{3-y} \cdot xReO_2$. The Raman spectra of the mixtures are shown in Fig. 6. All the observed vibrational modes in the frequency range from 20 to 900 cm^{-1}, for all the compositions, can be assigned to WO_3 dynamics. The Raman spectra in the mixtures with higher

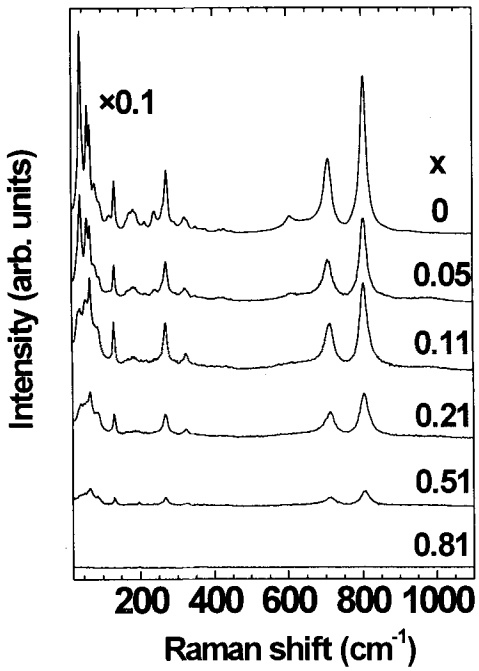

Fig. 6. Raman spectra (excited by the laser line 530.9 nm) of $(1-x)WO_{3-y} \cdot xReO_2$ mixtures. The intensity of the upper spectrum, corresponding to the *treated* WO_3 powder (x = 0) was reduced by a factor 10.

x seem rather similar to the spectra of pure WO_3 measured at temperatures well above the ambient one [27]. The addition of rhenium oxide does not induce any remarkable change in the spectral shape, like the appearance of new bands, except a weak band at 970 cm^{-1} discussed below. This fact suggests that no chemical reaction or formation of solid solution occur in the bulk of the crystal grains, and the ReO_2 phase is not Raman active. This is not surprising since rhenium ions in ReO_2 are located in highly symmetrical environments and the oxide has metallic conductivity: both facts reduce strongly the Raman activity.

The most striking effect observed in Raman spectra of these mixed powders is related to the strong quenching of the Raman scattering intensity upon increasing of the ReO_2 content. The presence of only 5 % of ReO_2 decreases drastically the total Raman intensity by a factor of about 20 (see difference in the intensity of spectra for x = 0 and x = 0.05 in Fig. 6). A further increase of the ReO_2 content in the range from 0.05 to 0.21 additionally lowers the intensity by a factor of two, and, finally, in the sample with x = 0.81 no appreciable Raman signal is observed. Note that the dramatic intensity decrease versus x cannot be justified by the decrease of the tungsten oxide content. Since all mixtures are coloured from greyish-blue

for low x values to black for high x values, and the colour was found to be stable against oxidising atmosphere, we suggest that the decrease of the Raman intensity is related to the formation of colour centres, similar to the case of ground WO_3 powders, with the reduced tungsten ions located at the tungsten oxide grain boundaries between WO_3 and ReO_2 phases. In fact, according to the electrical neutrality condition, the charge of the tungsten ions located at the boundaries between two phases should be lowered from 6+ to 5.7+, that transforms such sites into colour centres [11]. One can expect that the W-O bonds strength should be stronger for the reduced tungsten sites, as it was found in H_xWO_3 discussed above. Therefore, a high-frequency shift of the stretching Raman bands or an appearance of the new Raman band, associated with colour centres, can be expected: no shift of the 800 cm^{-1} band was observed, but the new band at about 950 cm^{-1} was detected (Fig. 7). To distinguish, if it is related to the colour centres, the Raman measurements using different laser wavelenghts were performed. As a result, the resonance Raman effect is observed for the 970 cm^{-1} band, when the excitation light approaches the absorption range (in the red) typical of these colour centres.

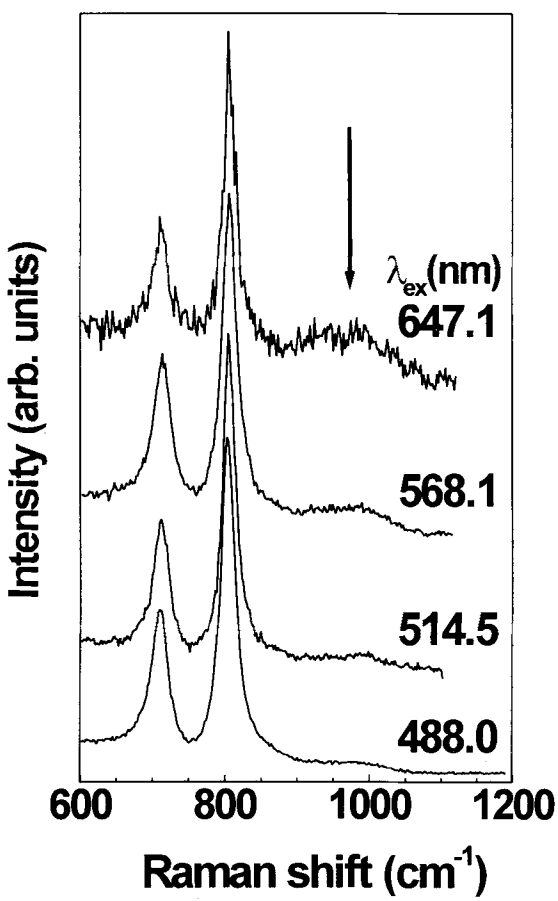

Fig. 7. Raman resonance effect for the band at ~ 970 cm^{-1} (indicated by arrow) in the mixed sample 0.95 WO_{3-y}·0.05 ReO_2. All spectra are normalized using the two strongest bands at 700 and 800 cm^{-1}. The wavelengths of the laser lines, used to excite the spectra, are also shown.

4. Conclusions

At high temperatures, the structural transformation occurring in pure WO_3 appears to be very similar to that controlled by the protons insertion in tungsten bronzes. It is observed that a symmetrization of the W-O bonds in WO_3 appears to occur gradually before reaching the tetragonal phase.

At low temperatures, the existance of tungsten oxide phases is strongly influenced by the mechanical history of the powders. The most striking effect is the transformation from monoclinic (I) to triclinic phase induced by moderate mechanical treatment like manual grinding for times on the scale of minutes. This transformation determines all the low-temperature evolution of the powder samples. Below RT the following two sequences can be proposed, on the basis of Raman spectra evolution at low temperature:

a) Untreated Powders: monoclinic (I) γ-phase exists between RT and ~ 220 K, whereas monoclinic (I) (gradually decreasing fraction upon cooling) and *N*-phase (increasing upon cooling) coexist between ~ 220 K and ~ 40 K (minimum explored temperature);

b) Treated powders: triclinic δ-phase prevails always between RT and ~ 70 K (minimum explored temperature) over small amount of *N*-phase, appearing below ~ 130 K.

Long duration milling induces an increasing structural disorder, but no amorphisation can be reached. XRD and Raman evidences of small amounts of the ε-phase, previously reported in bulk crystals only at low T, are found for 1 h milling duration.

A strong blue coloration of the powders increases together with the structural disorder upon the prolonged milling treatments. However, the coloration is reversible under the oxidising action of the atmosphere, and this bleaching process is strongly accelerated by moderate heating. The structural disordering, on the contrary, can be reversed only by high-temperature annealing (above ~ 300 °C). These findings are consistent with the hypothesis of electronic defects (colour centers) creation at the freshly generated surfaces during the milling process. The existance of such defects has some support by scanning tunneling microscopy [40,41].

In the mixtures $(1-x)WO_{3-y} \cdot xReO_2$, a permanent, non reversible coloration is obtained. In this case, the colour centres are related to reduced tungsten ions, distributed at the grain boundaries between the WO_3 and ReO_2 phases. The Raman band, attributed to such W-O bonds, exhibits some resonant behaviour when it is excited by red light, i.e. within the optical absorption band of the colour centres.

5. Acknowledgements

The authors would like to thank Mrs. C. Armellini for the help in the preparation of ground WO_3 samples and XRD measurements, Dr. E. Zanghellini for developing the soft-ware for Raman data analysis and for useful discussions, Dr. A. Veispals for the preparation of $(1-x)WO_{3-y} \cdot xReO_2$ mixtures. A.K. and J.P. are grateful to the Consiglio Nazionale delle Ricerche (Italy) and the Universita di Trento for hospitality and financial support.

6. References

[1] C.G. Granqvist, Handbook on Inorganic Electrochromic Materials. Elsevier Science, Amsterdam, 1995.

[2] V.E. Henrich and P.A. Cox, The Surface Science of Metal Oxides. Cambridge Univ. Press, Cambridge, 1994.

[3] S.K. Deb, Appl. Opt. Suppl. **3**, 192 (1969); S.K. Deb, Phil. Mag. **27**, 801 (1973).

[4] C.G. Granqvist, Appl. Phys. A **57**, 3 (1993).

[5] C.G. Granqvist, Solid State Ionics **53/56**, 479 (1992).

[6] C. Bechinger, D. Ebner, S. Herminghaus and P. Leiderer, Solid State Commun. **89**, 205 (1994).

[7] C. Bechinger, G. Oefinger, S. Herminghaus, P. Leiderer, J. Appl. Phys. **74**, 4527 (1993).

[8] I. Lefkowitz, M.B. Dowell and M.A. Shields, J. Solid State Chem. **15**, 24 (1975).

[9] E. Salje, A.F. Carley and M.W. Roberts, J. Solid State Chem. 29, 237 (1979).

[10] E. Cazzanelli, G. Mariotto, C. Vinegoni, A. Kuzmin and J. Purans, in: Electrochromic Materials and Their Applications III, (K.C. Ho, C.B. Greenberg, and D.M. MacArthur, Eds.) Proc. Electrochem. Soc. **96-24**, 260 (1996).

[11] A. Kuzmin, J. Purans, E. Cazzanelli, C. Vinegoni and G. Mariotto, J. Appl. Phys. **84**, 5515 (1998).

[12] J.B. Goodenough, Prog. Solid State Chem. **5**, 145 (1971).

[13] P.G. Dickens and R.J. Hurditch, Nature **251**, 1266 (1967).

[14] T. Iwai, J. Phys. Soc. Jpn. **15**, 1596 (1960).

[15] M. Kawaminami, and T. Hirose, J. Phys. Soc. Japan. **46**, 864 (1979).

[16] E.K.H. Salje, S. Rehmann, F. Pobell, D. Morris, K.S. Knight, T. Herrmannsdörfer and M.T. Dove, J. Phys.C: Condens. Matter **9**, (1997) 6563; E.K.H. Salje, Ferroelectrics **12**, 215 (1976)

[17] S. Tanisaki, J. Phys. Soc. Japan. **15**, 566 (1960).

[18] R. Diehl, G. Brand and E.K.H. Salje, Acta Crystallogr. B **34**, 1105 (1978).

[19] P.W. Woodward, A.W. Sleight, and T. Vogt, J. Phys. Chem. Solids **56**, 1305 (1995).

[20] B.O. Loopstra and P. Boldrini, Acta Crystallogr. B **21**, 158 (1966).

[21] B.O. Loopstra and H.M. Rietveld, Acta Crystallogr. B **25**, 1420 (1969).

[22] E.K.H. Salje, Acta Crystallogr. B **33**, 574 (1975).

[23] K.L. Kehl, R.G. Hay, and D. Wahl, J. Appl. Phys. **23**, 212 (1952).

[24] E. Cazzanelli, C. Vinegoni, G. Mariotto, A. Kuzmin and J. Purans, J. Solid State Chem. **143**, 24 (1999).

[25] P.G. Dickens, J.H. Moore and D.J. Neild, J. Solid State Chem. **7**, 241 (1973).

[26] C. Genin, A. Driouiche, B. Gerand and M. Figlarz, Solid State Ionics **53-56**, 315 (1992).

[27] E. Cazzanelli, C. Vinegoni, G. Mariotto, A. Kuzmin and J. Purans, Solid State Ionics **123**, 67 (1999).

[28] E.V. Gabrusenok, Sov. Phys. Solid State **26**, 2226 (1984).

[29] M.F. Daniel, B. Desbat, J.C. Lessegues, B. Gerand and M. Figlarz, J. Solid State Chem. **67**, 235 (1987).

[30] E.K.H. Salje, J. Appl. Cryst. **7**, 615 (1974).

[31] A. Kuzmin and J. Purans, J. Phys.C: Condens. Matter **5**, 2333 (1993).

[32] E.V. Gabrusenok, Lattice Dynamics of Tungsten Trioxide, in: Electrochromism. Reports of Latvian University, Latvian University, Riga, 1987, pp. 100-110.

[33] E.K.H. Salje and K. Viswanathan, Acta Crystallogr. A **31**, 356 (1975).

[34] E.K.H. Salje, Acta Crystallogr. A **31**, 360 (1975).

[35] M. Arai, S. Hayashi, K. Yamamoto and S.S. Kim, Solid State Commun. **75**, 613 (1990).

[36] S. Hayashi, H. Sugano, H. Arai and K. Yamamoto, J. Phys. Soc. Japan. **61**, 916 (1992).

[37] A. Anderson, Spectroscopy Lett. **9**, 809 (1976).

[38] T. Hirose, J. Phys.Soc. Japan. **49**, 562 (1980)

[39] J.V. Gabrusenoks, P.D. Cikmach, A.R. Lusis, J.J. Kleperis, G.M. Ramans, Solid State Ionics **14**, 25 (1984); M.F. Daniel, B. Desbat, J.C. Lassegues, R. Garie, J. Solid State Chem. **73**, 127 (1988); P. Delichere, P. Falaras, M. Froment, A. Hugot-Le Goff, Thin Solid Films **161**, 35 (1988); T. Nanba, Y. Nishiyama, I. Yasui, J. Mater. Res. **6**, 1324 (1991).

[40] F.H. Jones, K. Rawlings, J.S. Foord, R.G. Egdell, J.B. Pethica, B.M.R. Wanklyn, S.C. Parker and P.M. Oliver, Surf. Sci. **359**, 107 (1996); F.H. Jones, K. Rawlings, J.S. Foord, P.A. Cox, R.G. Egdell, J.B. Pethica and B.M.R. Wanklyn, Phys. Rev. B **52**, R14392 (1995)

[41] F.H. Jones, K. Rawlings, S.C. Parker, J.S. Foord, P.A. Cox, R.G. Egdell and J.B. Pethica, Surf. Sci. **336**, 181 (1995)

Paper presented at the 6th Euroconference on Solid State Ionics, Cetraro, Calabria, Italy, Sept. 12-19, 1999.

Manuscript rec. Oct. 7, 1999; acc. Nov. 30, 1999.